NUMERICAL SIMULATION OF THE INJECTION OF A POWERFUL ELECTRON BEAM INTO A VACUUM CHAMBER HAVING A STRONG MAGNETIC FIELD

Yu. A. Berezin, B. N. Breizman, and V. A. Vshivkov

UDC 533.916:517.949.8

The problem of beam transporting in a vacuum ranks high among the numerous problems associated with the use of powerful relativistic electron beams (REB) in physics experiments. Here it is analytically possible to consider only several of the simplest special cases; the majority of the situations require the use of numerical methods. The numerical procedures existing now are sufficiently effective for time-independent problems: they permit obtaining very high accuracy with totally acceptable expenditures of machine time [3-5]. Time-dependent problems are far more laborious and usually lie at the limit of possibilities of contemporary computational technique [6]. On the other hand, due to the comparatively short duration of powerful REB, time dependence often proves to be fundamentally important for them; in general it is necessary to take into account, along with the time dependence of the particle motion, the effects of retardation for the electric and magnetic fields. Since the corresponding calculations are very cumbersome, it is advisable to consider as the first step a situation in which the particle trajectories possibly appear more simply. This occurs upon the motion of the beam in a strong external magnetic field, when one can treat the particles as "strung" onto the force lines. This is precisely the case which is discussed in this paper. We note that the indicated formulation of the problem is sufficiently realistic, since in many experimental setups a strong field is created which predetermines the appearance of the electron trajectories.

1. The experimental scheme under discussion for transporting an REB is of the following form. The beam enters a cylindrical vacuum chamber through the anode foil, which is located at the end of the cylinder. Passing through the drift space, the beam is incident on the other end, which is the collector. The chamber walls, the foil, and the collector are at zero potential. An external magnetic field is uniform in the direction along the chamber axis (it is understood that the entire system possesses axial symmetry).

We will represent the beam in the drift chamber in the form of a set of tubular beams, each of which has a negligibly small thickness and can be taken into account as a boundary condition in the solution of Maxwell's equations. By properly specifying the number of tubular beams, their currents, and their radii, one can actually model an arbitrary distribution of injected current. For simplicity's sake we will formulate the problem for the case in which only one current tube occurs in all.

In cylindrical coordinates (r, z) the drift space has a triangular form $0 \leqslant r \leqslant R$, $0 \leqslant z \leqslant L$. The current tube divides this region into two subregions: I ($0 \leqslant r \leqslant r_b$) and II ($r_b \leqslant r \leqslant R$).

In view of the axial symmetry of the problem, the system of Maxwell's equations is split into two independent systems (for TE- and TM-waves). The beam affects only the TM-waves in which the quantities E_r, E_z, and H_φ are different from zero:

$$\frac{\partial E_r}{\partial t} = -c\frac{\partial H_\varphi}{\partial z}; \tag{1.1}$$

$$\frac{\partial E_z}{\partial t} = \frac{c}{r}\frac{\partial}{\partial r}(rH_\varphi); \tag{1.2}$$

$$\frac{\partial H_\varphi}{\partial t} = c\left(\frac{\partial E_z}{\partial r} - \frac{\partial E_r}{\partial z}\right). \tag{1.3}$$

The boundary conditions on the walls of the drift chamber are of the form

$$E_z = 0 \text{ at } r = R,\ H_\varphi = E_r = 0 \text{ at } r = 0,$$
$$E_r = 0 \text{ at } z = 0 \text{ and } z = L.$$

Novosibirsk. Translated from Zhurnal Prikladnoi Mekhaniki i Tekhnicheskoi Fiziki, No. 1, pp. 3-9, January-February, 1981. Original article submitted January 10, 1980.

0021-8944/81/2201-0001$07.50

It is necessary to supplement these formulas by matching the fields at $r = r_b$ (on the beam):

$$E_r^{II} - E_r^I = 4\pi\sigma, \quad H_\varphi^{II} - H_\varphi^I = \frac{4\pi}{c} j. \tag{1.4}$$

Here $\sigma(z, t)$ and $j(z, t)$ are the surface charge and current densities. The function E_z is continuous at $r = r_b$ ($E_z^{II} = E_z^I$), and its derivative with respect to the radius undergoes a discontinuity:

$$\frac{\partial E_z^{II}}{\partial r} - \frac{\partial E_z^I}{\partial r} = \frac{4\pi}{c^2}\frac{\partial j}{\partial t} + 4\pi\frac{\partial \sigma}{\partial z}. \tag{1.5}$$

We determine the variation of the charge density and current by proceeding from the equations of motion of the electrons:

$$\frac{d}{dt}\left(\frac{m_e v}{\sqrt{1 - v^2/c^2}}\right) = -eE_z(r_b, z, t), \quad \frac{dz}{dt} = v.$$

The total energy of the system W is comprised of the energy of the electromagnetic field

$$W_1 = \int\int \frac{r}{4}\left(E_r^2 + E_z^2 + H_\varphi^2\right) dr dz$$

and the kinetic energy of the electrons

$$W_2 = -\frac{2\pi m_e c^2}{e} r_b \int \gamma\sigma dz,$$

where $\gamma = (1 - v^2/c^2)^{-1/2}$. The variation of W is related solely to the fact that the electrons cross the boundaries of the region $0 \leqslant z \leqslant L$:

$$\frac{dW}{dt} = \frac{2\pi m_e c^2}{e} r_b \left[(v\gamma\sigma)_{z=L} - (v\gamma\sigma)_{z=0}\right]. \tag{1.6}$$

Equation (1.6) will be used in the following as a control on the computational accuracy.

2. A scheme with overstepping is used for the numerical solution of Eqs. (1.1)-(1.3). For this purpose the functions E_r, E_z, and H_φ are specified on grids shifted relative to each other. The values of the functions E_r and H_φ on the beam are determined from Maxwell's equations with the boundary conditions (1.4) and (1.5) taken into account. The method of particles in cells is used to solve the equations of motion. The surface charge and current density necessary in conditions (1.4) and (1.5) are determined from the positions and velocities. The indicated algorithm is outlined in detail in [7].

The initial conditions were specified as follows in all the calculated versions. At the initial instant of time the functions E_r, E_z, and H_φ are equal to zero and there are no particles in the drift space. Then at each time step an identical number of particles enters the drift space through the boundary $z = 0$ in order to provide a constant injected current.

3. Systematic calculations were performed in order to check the accuracy of this algorithm. One of them was the following. The injected current is increased very slowly from zero to some value I_0. The system arrived at a state differing little from the steady state which exists for a given value of the current. The parameters of the problem were as follows: $I_0 = 0.03I_*$, $v_0 = 0.9c$, $r_b = 0.4R$, $L = 5R$, $h_r = h_z = 0.1R$, $\tau = 0.01R/c$, and 2000 particles. Here and later the current is measured in units of the critical vacuum current I_* for a tubular beam in an infinitely long system [8]

$$I_* = \frac{(m_e c^3/2e)}{\ln(R/r_b)}\left(\gamma_0^{2/3} - 1\right)^{3/2}, \tag{3.1}$$

where $\gamma_0 = (1 - v_0^2/c^2)^{-1/2}$. The injected current increases linearly in a time $t \approx 22R/c$, and at the time $t = 30R/c$ the deviation of all the quantities (I, v, σ) at the middle of the beam from the values of the steady solution did not exceed 0.05%. The deviation of the total energy from the values of the steady solution was 0.052% at this very same time.

The accuracy was controlled in the computational process by checking fulfillment of the law of conservation of energy. For this purpose the energy $W_0(t)$ which the system should have up to time t is calculated. It is calculated by integrating Eq. (1.6) over the time. On the other hand, the energy can be calculated as the sum of the quantities W_1 and W_2 (see Sec. 1). The discrepancy between the energies calculated by these two methods is a measure of the computational accuracy.

TABLE 1

$t(R/c)$	$\tau=0,05R/c$	$\tau=0,025\ R/c$	$\tau=0,01R/c$
5	$\delta W=1,28\%$	1,21	1,21
10	1,24	1,22	1,24
15	1,26	1,24	1,24
20	1,35	1,24	1,24
25	1,74	1,28	1,25

TABLE 2

I_0/I_*	1,06	1,12	1,18	1,30
$\bar{z}(R)$	0,84	0,64	0,54	0,48

The calculations have shown that the accuracy increases when the steps are reduced. For example, in a calculation with $I = 0.6I_*$ ($L = 5R$, $v_0 = 0.9c$, $\tau = 0.025R/c$, and 2000 particles) the relative deviation of the energy at time $t = 10R/c$

$$\delta W = \frac{W(t) - W_0(t)}{W_0(t)},$$

where $W(t) = W_1(t) + W_2(t)$, is equal to $\delta W = 1.22\%$ with $h_z = h_r = 0.1R$ and $\delta W = 0.64\%$ with $h_z = h_r = 0.05R$.

The effect of the time step on the computational accuracy is shown in Table 1, which is compiled from computational results having the very same parameters as in the preceding example ($h_z = h_r = 0.1R$). It is evident from Table 1 that the computational accuracy remains approximately constant for different steps τ, i.e., it is determined by the spatial steps in this version. But the smaller the step τ is, the longer this accuracy is preserved.

4. Let us discuss the passage of a tubular current through a cylindrical chamber.

Depending upon the value of the injected current, two modes of motion existed. With a small current the beam passed through the drift space experiencing together with the electromagnetic field periodic oscillations about the average values. These oscillations amount to 10-15% of the average values in size and are related to the fact that the injected current has a sharp leading edge. As a result of this injection, electromagnetic waves are excited in the chamber which do not die out with time. This mode was observed up to certain critical values. Since the chamber has a limited length, the value of the critical current is larger for it than that calculated from Eq. (3.1). The greater the difference, the shorter the chamber. Thus for $L = 5R$ the critical current was larger than I_* by 0.8%, and for $L = R$ the critical current exceeded I_* by a factor of 1.9 (in both cases $r_b = 0.4R$, and $v_0 = 0.9c$).

Starting from the critical current, the nature of the motion is altered. When the current exceeds I_* by a small amount, the leading front of the beam passes through the drift space without particle reflection. Gradually, a charge is accumulated in the system, and part of the electrons start to be reflected starting from some time. As time passes, the point at which particle reflection occurs (the virtual cathode) is shifted towards the beginning of the chamber. The system arrives at a quasisteady state. The final position of the reflection point z depends upon the value of the injected current I_0: the larger the current is, the nearer this point is located towards the front of the chamber (Table 2).

With large injected currents particle reflection starts at earlier times. The nature of the motion remains the same. The position of the particles in the plane (z, $p = \gamma v/c$) at times $t = 2$, 4, 6, 8, and 10 is given in Figs. 1 and 2; the lines parallel to the horizontal axis denote different velocities in units of the speed of light. The corresponding values of the velocity are indicated on the right. These calculations were done for an injected current $I = 1.78I_*$ ($L = 5R$, $r_b = 0.4R$, $v_0 = 0.9c$), and the time t is indicated in units of R/c. All the effects which we have spoken about above are readily visible on these graphs. The graphs in Fig. 2 differ little from each other, which indicates the production of quasisteady conditions. The current passing through is greater than I_* by 0.84% here. The computing time for this version was 7 min on a BÉSM-6. The computational grid had 20 nodes along the radius

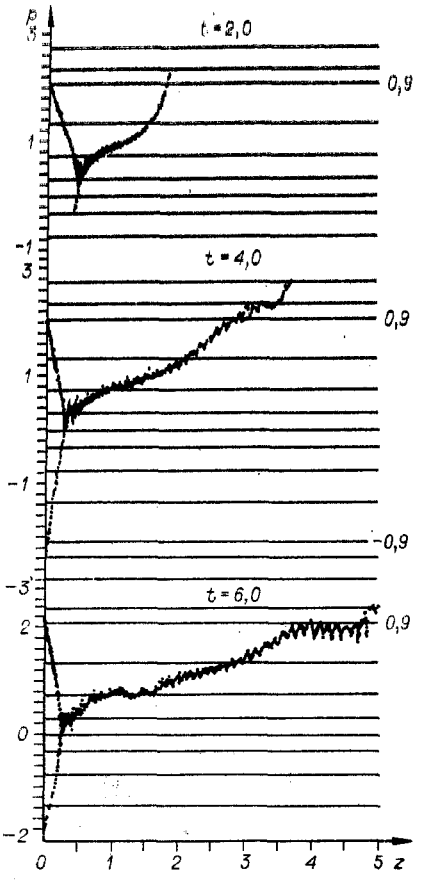

Fig. 1

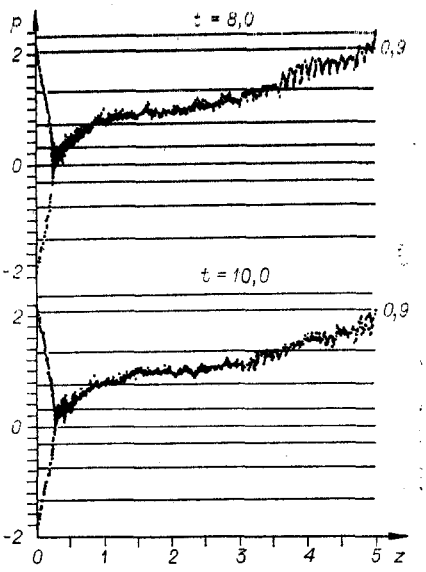

Fig. 2

and 100 nodes along the length. A total of 400 steps in the time were made. The number of particles in the drift space at time 10R/c was equal to 1727.

The ratio max $|\mathrm{rot}\,\mathbf{E}|/\max|\mathbf{E}/R|$ at various times was calculated in this version. It varied within the range from 1.2 to 5.8, which indicates that the non-potential part of the electric field is of the very same order of magnitude as in the field itself. Consequently, taking electromagnetic effects into account is necessary for the correct solution of the problem.

5. Let us consider a tubular beam in a chamber of variable cross section. It was assumed in these calculations that the chamber radius varies in a stepwise fashion. As an example, let us consider the calculation of the motion of the beam in the drift space illustrated in Fig. 3. The beam radius is $r_b = 0.2R$, and the injection velocity is $v_e = 0.9c$. The injected current was selected in such a way that it was subcritical $I = 0.9I_*^1$ in the smaller section and supercritical $I = 1.5I_*^2$ in the larger one. Here I_*^1 and I_*^2 are the critical currents for the small and large sections of the chamber. The phase planes (z, p) at different times for this calculation are given in Fig. 4. The vertical line on the graphs denotes the position of the discontinuity in the cross section of the chamber. It is evident from Fig. 4 that the beam passes freely through the chamber with the smaller radius and starts to be reflected in the region having the larger cross section at the point $z = 1.7R$. The reflected part of the beam together with the injected beam produces a charge in the region having the smaller cross section which is sufficient for reflection in this section. Therefore the virtual cathode is shifted as time passes into the region having the smaller cross section, approaching $z = 0.3R$.

6. Let us discuss opposed beams in a cylindrical chamber. The phase pattern corresponding to injection into the drift chamber of two indentical opposed beams is given in Fig. 5. The current of each of the beams is $(2/3)I_*$, so that the total volume charge corresponds to a current of $(4/3)I_*$ ($L = 5R$, $r_b = 0.4R$, $v_e = 0.9c$). Therefore, particle reflection is observed in the system. The calculation has shown that charge accumulation occurs slowly, and particle reflection starts only at the time $t = 13R/c$. Then the pattern on the phase

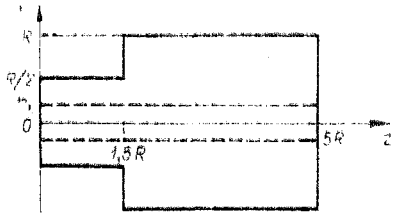

Fig. 3

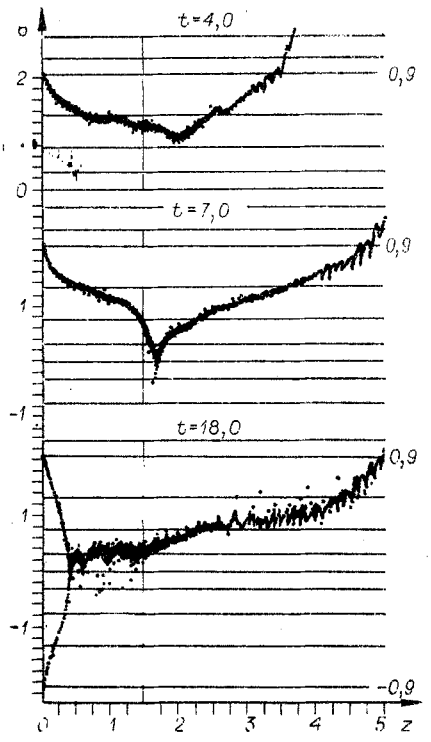

Fig. 4

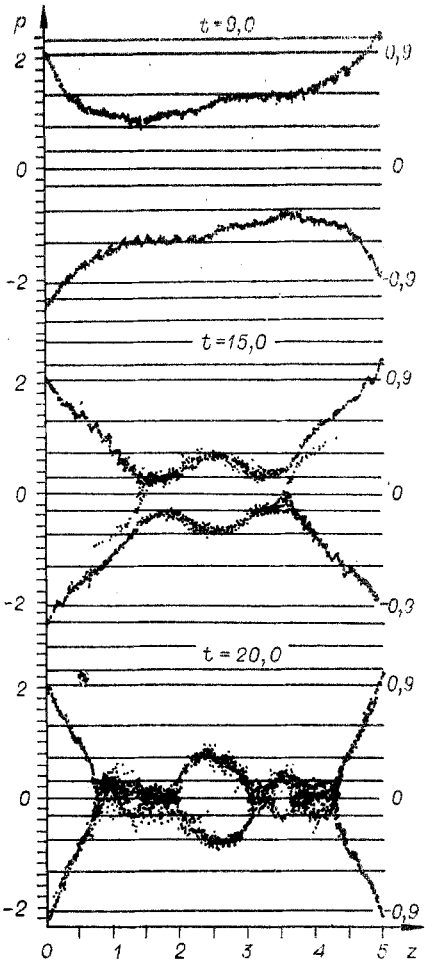

Fig. 5

plane becomes quasisteady. Starting from t = 17R/c, it changes hardly at all (the calculation was performed out to the time t = 25R/c).

A similar calculation for small injection currents ($I < 0.5I_*$) shows that both beams pass through the chamber without reflection in this case, as should be expected. We note that the particle motion in the chamber proves to be stable.

As was already stated above, one can use several tubular beams embedded one within the other to simulate a beam with the current distributed over the cross section. The calculations are performed with eight beams embedded one within the other. The surface density of the injection current was taken to be identical in all the beams $j_k = j_0$ (k = 1, ..., 8) in order to produce a current density uniform over the cross section. The beams were located in the first eight radial nodes from the axis. This calculation showed that reflection occurs more strongly in the inner beams than in the outer one and the part of the beam which reaches the collector has in fact a tubular cross section.

It is evident from the examples given that the algorithm of [7] offers the possibility of investigating rather complicated combinations of drift space and beam arrangement.

LITERATURE CITED

1. G. Vallis, K. Zauer, et al., "The injection of high-current relativistic electron beams into plasma and gas," Usp. Fiz. Nauk, 113, No. 3 (1974).
2. B. N. Breizman (Brejzman) and D. D. Ryutov, "Powerful relativistic electron beams in a plasma and in a vacuum (theory)," Nucl. Fusion, 14, 873-907 (1974).
3. V. P. Il'in, Numerical Methods for Solution of Electrooptical Problems [in Russian], Nauka, Novosibirsk (1974).
4. J. W. Poukey, J. R. Feeeman, and G. Yonas, "Simulation of relativistic electron beam diodes," J. Vac. Sci. Technol., 10, No. 6 (1973).
5. A. A. Kolomenskii and M. A. Novitskii, "A two-dimensional model of the propagation of a high-current electron beam and the acceleration of ions from a gas," Zh. Tekh. Fiz., 46, No. 1 (1976).
6. J. P. Boris, "Relativistic plasma simulation—optimization of a hybrid code," in: Fourth Conf. on Numerical Simulation of Plasmas, Washington (1970).
7. V. A. Vshivkov, "Numerical simulation of a relativistic electron beam," Chislennye Metody Mekh. Sploshnoi Sredy, 10, No. 2 (1979).
8. D. D. Ryutov, "The critical vacuum current of relativistic electron beams," Zh. Tekh. Fiz., 47, No. 4 (1977).

TRANSVERSE OSCILLATIONS IN A PARTIALLY COMPENSATED ELECTRON BEAM

A. S. Chikhachev

UDC 533.9

Discussion of the motion of not only electrons but also ions of a beam is significant in connection with the investigation of the problem of the stability of a quasisteady quasirelativistic beam. Instabilities of a beam partially compensated with respect to deflection (instabilities of the "snake" type) are discussed in [1]. A model of two filaments formed by electrons and ions of a beam which can shift relative to each other was used. The structure of the beams in phase space is not important for the problems investigated in [1] — the transverse oscillations are analyzed from the motion of axial particles.

The stability of an electron—ion beam relative to axisymmetric perturbations of the radii of the electron and ion components is discussed in this paper. We will assume that both the electrons and the ions of the beam are characterized by a nonzero emittance.

1. It is necessary in connection with the description of the beam particles with the help of a distribution function in the nonsteady case to find an integral of the motion which is not a consequence of the uniformity of the system, which is possible in the paraxial approximation [2, 3].

We will seek the electron distribution function in the form

$$f_e = \varkappa\delta(I - I_{0e})\ \delta(\beta_z - \beta_0), \tag{1.1}$$

where $\varkappa$ is a normalization constant; $\beta_z = v_z/c$; v_z, longitudinal velocity of the electrons; c, speed of light; and I, a functional which depends on the transverse coordinates and velocities.

Satsifaction of the condition $J \ll \gamma\beta_0 mc^3/e$, where J is the total current of the beam, e and m are the charge and mass of the electron, and γ is a relativistic factor, is necessary for the validity of (1.1). The quantity β_z is an approximate integral of the motion which is a consequence of conservation of the z-component of the generalized momentum.

One can represent the function I in the case of an axisymmetric beam under discussion in the form

$$I = A_e(t)\left[\left(\dot{r} - \frac{\dot{A}_e r}{2A_e}\right)^2 + \frac{C_{0e}^2}{r^2}\right] + \frac{E_{0e}^2}{A_e(t)}r^2, \tag{1.2}$$

Moscow. Translated from Zhurnal Prikladnoi Mekhaniki i Tekhnicheskoi Fiziki, No. 1, pp. 9-15, January-February, 1981. Original article submitted October 15, 1979.

0021-8944/81/2201-0006$07.50